ISIJ International, Vol. 57 (2017), No. 7, pp. 1282–1288

Two Step Ductile to Brittle Transition Behavior on Ferrite + Pearlite Structure Steel Sheet

Hiroyuki KAWATA[1)]* and Osamu UMEZAWA[2)]

1) Steel Research Laboratories, Nippon Steel and Sumitomo Metal Corporation, 20-1 Shintomi, Futtsu, Chiba, 293-8511 Japan. 2) Faculty of Engineering, Yokohama National University, 79-5 Tokiwadai, Hodogaya-ku, Yokohama, Kanagawa, 240-8501 Japan.

(*Received on January 13, 2017; accepted on March 21, 2017; J-STAGE Advance published date: May 24, 2017*)

Although a few studies on the fracture behavior of dual phase (DP) steels have been conducted, the mechanism of impact fracture in DP steels has not yet been clarified. In this study, the ductile to brittle transition behavior in ferrite + pearlite DP steel sheets was evaluated using the Charpy impact test with a sub-size specimen. The absorbed energy of DP steel decreased with decreasing temperature and the transition curve had a clear "middle shelf" existing between upper and lower shelves. The fracture surface at the middle shelf was flat and contained few dimples, similar to that at the lower shelf. Ferrite grains just below the fracture surface obviously received plastic strain with fracture on the middle shelf. This result indicated that the fracture mode on the middle shelf was quasi-cleavage fracture (QCF). Furthermore, on the lower shelf, ferrite grains received very small plastic strain with fracture. The two step ductile to brittle transition in this study corresponded to the fracture mode that changed from microvoid coalescence fracture to QCF and from QCF to cleavage fracture.

KEY WORDS: ductile to brittle transition; dual phase steel sheet; Charpy impact test; cleavage fracture; quasi-cleavage fracture.

1. Introduction

High strength steels containing multiple phase structures that show advanced performances are highly desired. For example, dual phase (DP) steel consisting of soft ferrite and hard structure, such as martensite, bainite, or pearlite, exhibits high strength and good formability, and it is widely used for automobiles.[1)] However, there is a limitation for the applications of high strength materials owing to their poor fracture properties. Several studies on the fracture behavior of DP steels have been conducted with particular focus on tensile,[2–5)] fatigue,[5,6)] and hydrogen embrittlement.[7,8)]

On the other hand, regarding the impact fracture, the influence of the volume fraction of martensite on the impact absorbed energy[9,10)] has been evaluated along with the effect of tempering.[9)] The effect of grain size on ductile to brittle transition (DBT) behavior[11)] was also investigated. Although these studies pointed out the microstructural effect on impact fracture properties, information regarding the mechanism in DP steels is limited.

The specimen thickness is the most important factor for the evaluation of impact fracture using the Charpy impact test.[12–14)] DP microstructure is mainly applied for sheet steels that are thinner than full-size Charpy impact specimens (10 mm). Therefore, the inspection of the impact fracture behavior on DP steels with a sub-size specimen is required. In this study, we focused on DBT behavior and features of fracture surfaces on DP steel sheets consisting of soft ferrite and hard pearlite.

2. Experimental Procedure

2.1. Material

The ferrite + pearlite DP steel sheet was prepared at the laboratory scale. The chemical compositions of the steel sheet used was 0.15 C – 1.77 Si – 1.48 Mn – 0.005 P – 0.001 S – 0.001 N in mass%. The ingot melted by a vacuum induction furnace was hot-rolled over 1 173 K to a thickness of 2.5 mm and air-cooled to room temperature. After hot-rolling, to prepare the ferrite + pearlite structure, the sheet was heated at 1 033 K, air-cooled until 873 K, held at 873 K for 1 hour and water quenched.

Figure 1 shows the SEM image of the microstructure etched by nital in the steel sheet. In this image, ferrite grains (α) and pearlite islands (P) were observed. The shape of the ferrite grains is mainly polygonal, and the average diameter is 14 μm. Pearlite islands exist between ferrite grains, and the volume fraction of pearlite evaluated using the point counting method is 15%. The tensile properties of this steel sheet were measured with a 50 mm strain gage. The 0.2% proof stress, tensile strength, and elongation are 385 MPa, 595 MPa, and 31%, respectively.

* Corresponding author: E-mail: kawata.z84.hiroyuki@jp.nssmc.com
DOI: http://dx.doi.org/10.2355/isijinternational.ISIJINT-2017-026

2.2. Charpy Impact Test

We evaluated DBT behavior using the Charpy impact test with a sub-size specimen between 77 and 353 K. **Figure 2** shows the schematic of the sub-size Charpy impact test specimen used. Its length was 55 mm parallel to the transverse direction (TD) and its width was 10 mm along the rolling direction (RD). Moreover, the thickness of the steel sheet was 2.5 mm. A 2 mm V-notch was cut on center of the specimen. The input energy of this test was 300 J. The temperature was controlled by a thermocouple welded on the specimen surface. The specimens were immersed in hot water or denatured alcohol maintained at temperatures between 173 and 353 K. Below 153 K, the specimens were first immersed in liquid nitrogen and then taken out. The specimens were subsequently tested after they reached the target temperature.

2.3. Fracture Surface Analysis

After the impact test, we observed fracture surfaces via field-emission scanning electron microscope (FE-SEM, JEOL–6500F). To clarify the fracture mode, we observed the microstructure just below the fracture surface at 1/2 thickness of some specimens using the electron back-scattering diffraction (EBSD) technique[15] in the nominal direction (ND). Moreover, the grain orientation spread (GOS) values in each ferrite grain were calculated from EBSD data. The GOS value is the average misorientation among all pixels within a grain surrounded by a high angle boundary ($\geq 10°$). This value is very small in ferrite grains without strain and increases with plastic deformation.[16]

3. Results

3.1. Impact Energy

Figure 3 shows the fractographs of the specimens that failed at 323 and 153 K. At 323 K, Fig. 3(a), almost all the fracture surface was covered with small dimples. This is a typical ductile fracture surface, which is called the microvoid coalescence fracture[17] surface (MVCFS). Figure 3(b) shows that there is no or small amount of dimples on the fracture surface failed at 153 K. This surface is a typical brittle fracture surface. In macroscopic view, this surface is very flat; therefore, it is easy to distinguish between this surface and MVCFS. We call this flat surface "low energy fracture surface (LEFS)."

From Fig. 3, it is observed that the energy transition between 323 and 153 K is DBT. **Figure 4** shows the impact energy transition behavior of ferrite + pearlite DP steel sheets. The impact energy decreased severely with decreasing temperature from 323 to 173 K. However, the shape of the transition curve was different from the conventional curve of BCC steel.[18] In general, the DBT curve is described with the upper shelf having large absorbed energy and the lower shelf having small absorbed energy. On the general DBT behavior, the energy moves continuously between the two shelves. However, in this case, as seen in Fig. 4, the curve between the upper and lower shelf is not smooth. The absorbed energy in this study decreases from 1 270 to 630 kJ/m^2 between 323 and 253 K. More-

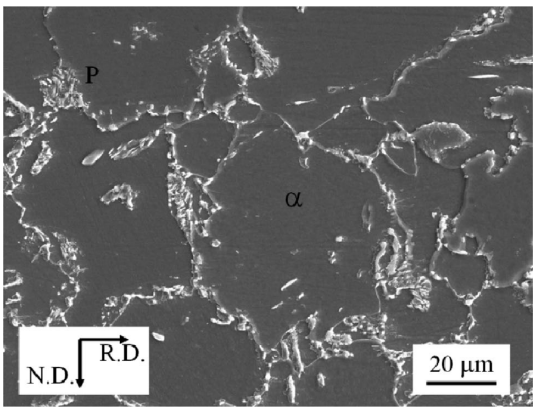

Fig. 1. Microstructure of the ferrite + pearlite steel sheet used in the TD section.

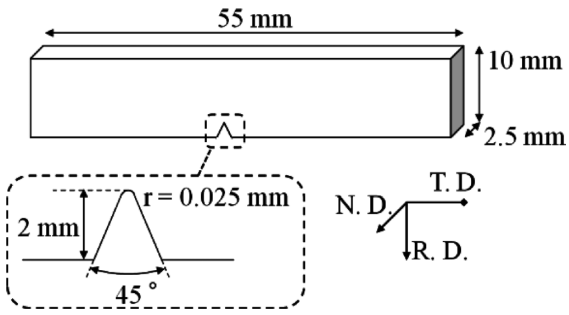

Fig. 2. Schematic of a sub-size Charpy impact test specimen.

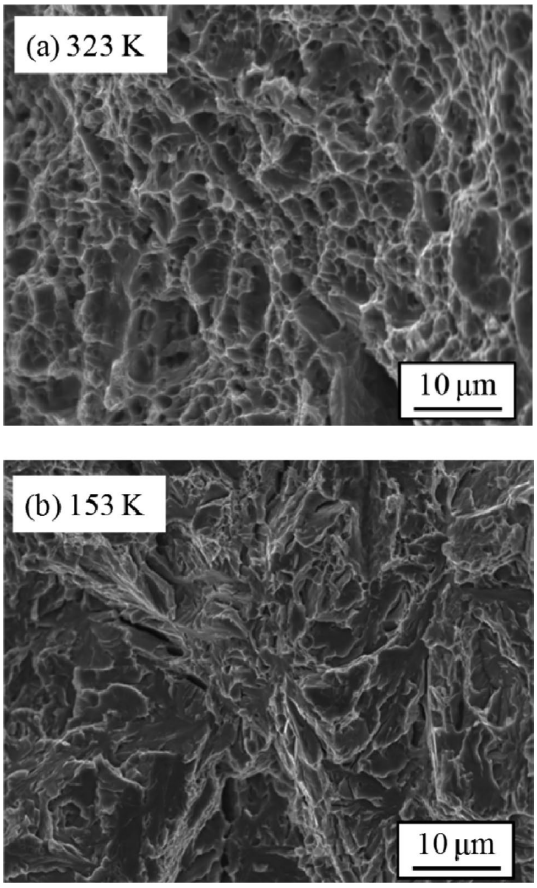

Fig. 3. Magnified images of the fracture surfaces at the 1/2 thickness of ferrite + pearlite steel sheet tested at (a) 323 and (b) 153 K.

over, between 253 and 193 K, the energy decreases gradually from 630 to 530 kJ/m^2. Finally, the energy transition appears clearly from 193 to 173 K. The DBT in this study is observed to occur with two steps, and there is a "middle shelf"[19] between the upper and lower shelf. Moreover, the width of the middle shelf range is over 60 K. We call the transition from the upper shelf to the middle shelf as "first transition" and the transition from the middle shelf to the lower shelf as "second transition."

3.2. Fractography

Figure 5 shows the macroscopic fractographs of sub-size Charpy specimens tested between 323 and 153 K. V-notch existed on the upper side in each fractograph; therefore, the fracture propagated from up to down. Figure 5(a) shows that the fracture surface failed at 323 K on the upper shelf, and is completely covered by typical ductile fracture surface, MVCFS, which is observed in Fig. 4(a). Furthermore, the fracture surface failed at 295 K (Fig. 5(b)) is a mixed surface of MVCFS and LEFS, which is observed on the brittle fracture specimen in Fig. 4(b). Figure 5(c) shows the sketch of the fracture surface failed at 295 K, and black line corresponds to the edge of the fracture surface. In this sketch, the white layer is the ductile fracture surface, MVCFS, and the gray layer is the flat fracture surface, LEFS. In this sample, the area fraction of LEFS over the fracture surface is 34%. On the middle shelf, the fracture surface failed at 213 K (Fig. 5(d)) is almost covered by LEFS. This feature is similar to that on the lower shelf at 153 K (Fig. 5(e)). There are very small areas of MVCFS around the edge of the fracture surface.

Figure 6 shows the fracture surface transition of a ferrite + pearlite steel sheet. The fraction of LEFS on the entire fracture surface increases during first transition from the upper shelf to the middle shelf. On the middle shelf, the fraction of LEFS is over 95%, as observed in Fig. 5(d). Therefore, it is impossible to notice the second transition by macroscopic fractographs.

Figure 7 shows details of the fracture surface failed at

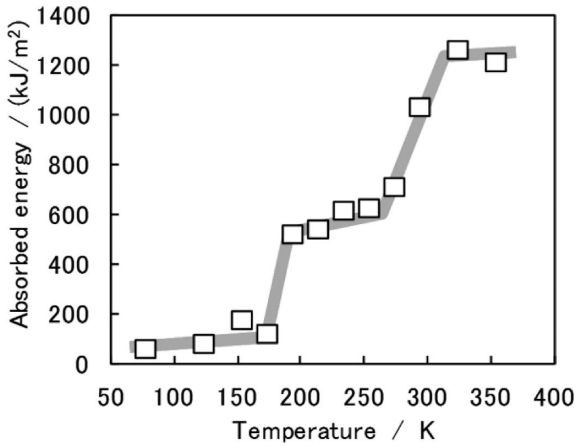

Fig. 4. Energy transition of the ferrite + pearlite steel sheet using a sub-size Charpy impact test specimen.

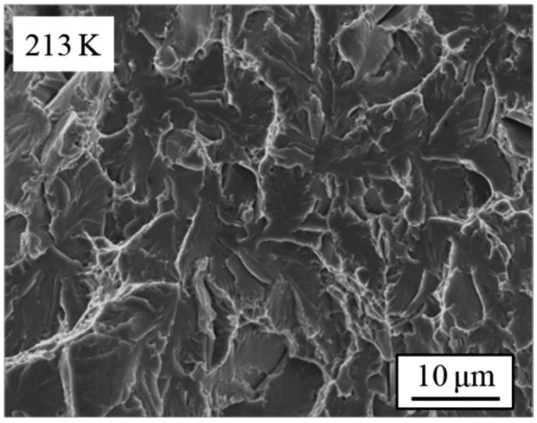

Fig. 6. Magnified image of the fracture surface at the 1/2 thickness of ferrite + pearlite steel sheet tested at 213 K.

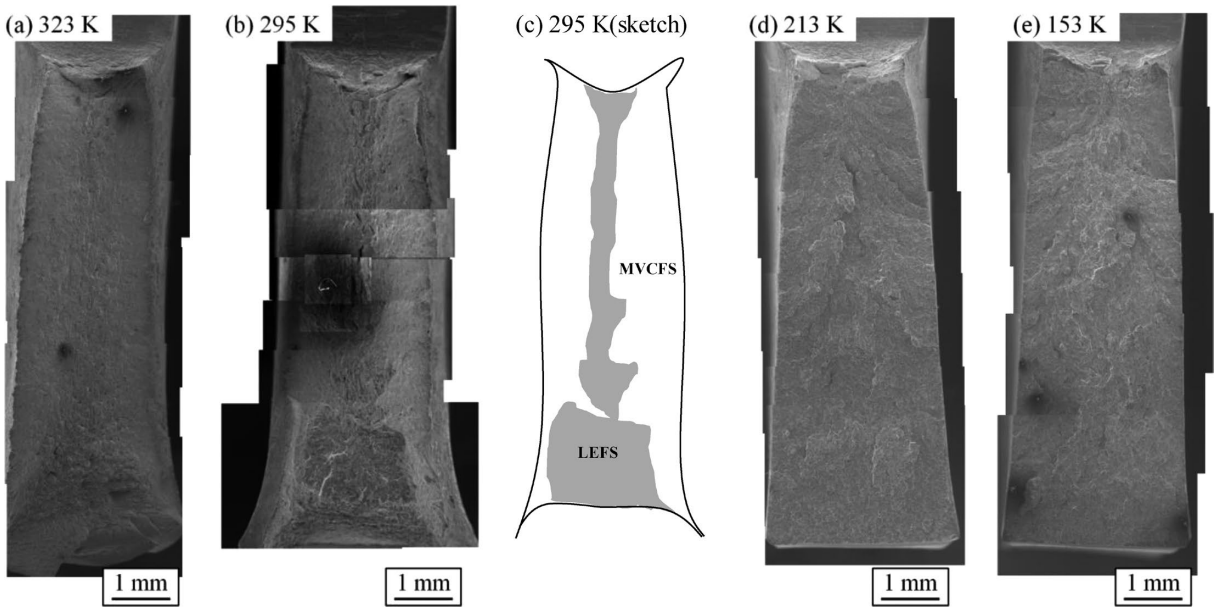

Fig. 5. Fracture appearance of sub-size Charpy impact specimens tested at (a) 323, (b) 295, (d) 213, and (e) 153 K. Sketch of the fracture surface (c) is illustrated in photograph (b). MVCFS (white layer): microvoid coalescence fracture surface and LEFS (gray layer): low energy fracture surface.

213 K on the middle shelf. The surface containing few dimples and other features of ductile fracture is very similar to that failed on the lower shelf (Fig. 4(b)). Therefore, it is impossible to distinguish between the fracture surface on the middle shelf and that on the lower shelf by fractographs.

3.3. Crystallographic Features Just Below the Fracture Surface

To clarify the mechanism of two step DBT behavior, we observed the microstructure just below the fracture surface using the EBSD technique. **Figure 8**(a) shows a BCC inverse pole figure (IPF) map of the sample material without impact test. Black lines correspond to grain boundaries whose rotation angles are >10°. The microstructure of ferrite + pearlite steel sheet consists of equiaxial ferrite grains and pearlite islands, as observed in Fig. 1. Moreover, some pearlite islands arrowed in Fig. 8(a) contain ferrite lamellar, whose crystallographic orientations are near the neighboring ferrite grains. Figure 8(b) shows the crystallographic orientation deviations into each ferrite grain. Before impact test, ferrite grains have very small deviations in themselves.

Figure 9(a) shows the IPF map of the region just below the fracture surface of a sub-size Charpy specimen failed at 153 K on the lower shelf. The upper tip of this map is the fracture surface. The left side is the notch side; therefore, the fracture propagated from left to right in this map. Black lines correspond to high angle boundaries (≥10°), and gray lines correspond to low angle boundaries (≥2°). This map

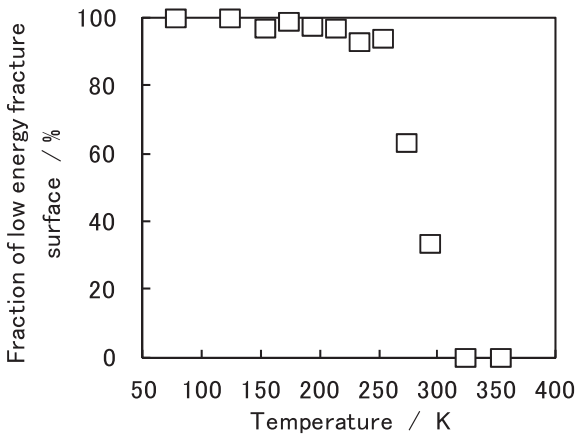

Fig. 7. Fracture surface transition of ferrite + pearlite steel sheet using a sub-size Charpy impact test specimen.

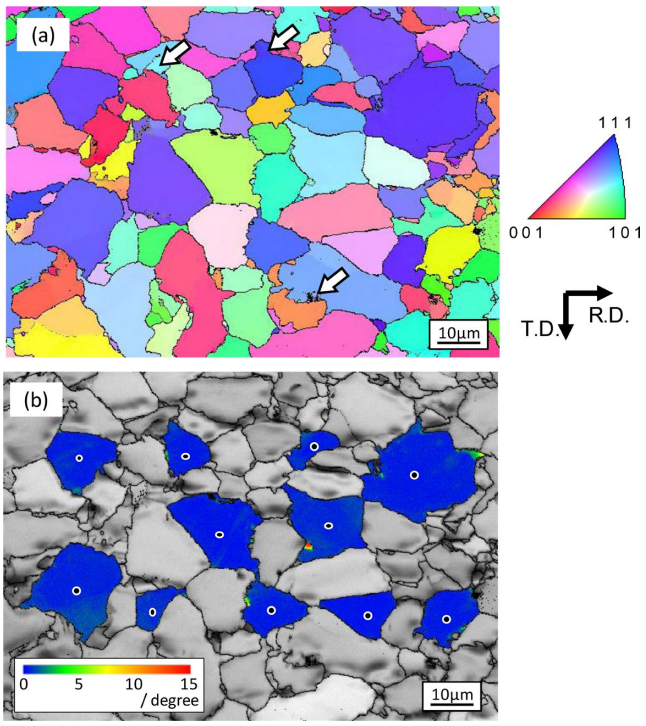

Fig. 8. Orientation image of the ferrite + pearlite steel sheet. (a) inverse pole figure (IPF) map of ND and (b) misorientation from standard point (●) in each ferrite grain. (Online version in color.)

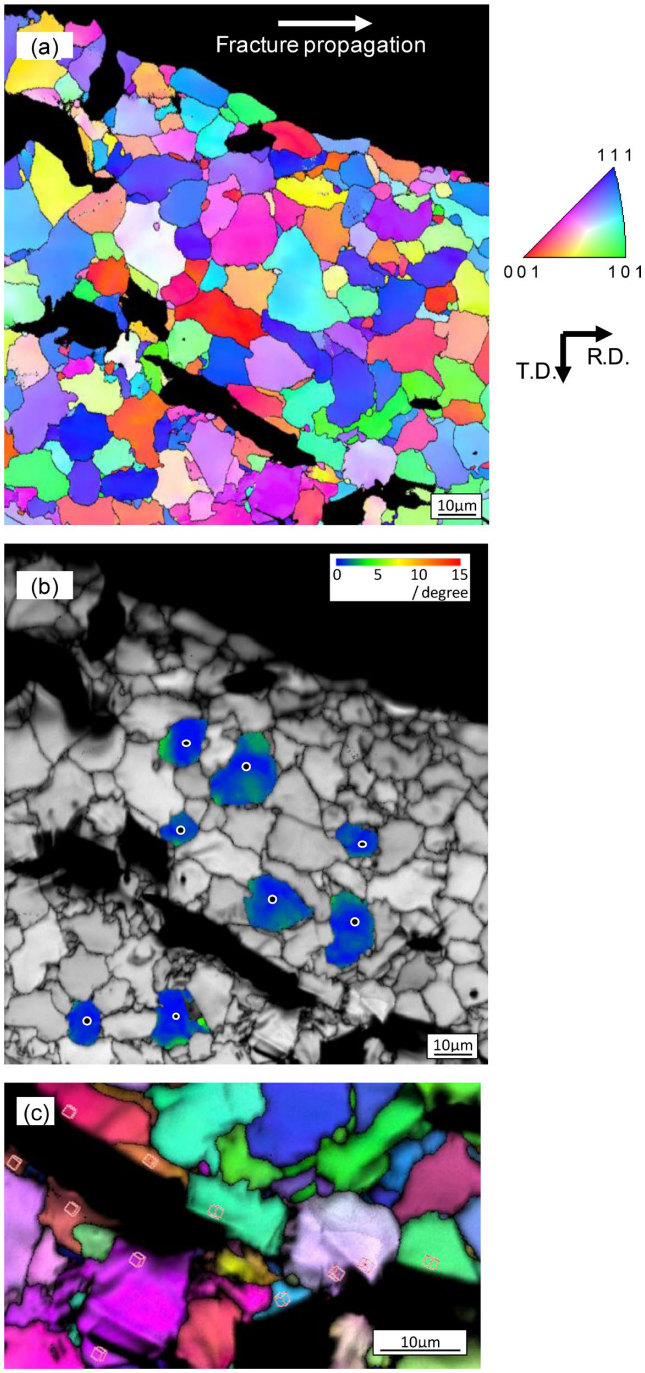

Fig. 9. Orientation image of the ferrite + pearlite steel sheet failed at 153 K in the cross section below the low energy fracture surface. (a) IPF map of ND, (b) misorientation from standard point (●) in each ferrite grain, and (c) microcracks in ferrite grains. (Online version in color.)

looks similar to the initial structure (Fig. 8(a)), except for cracks. Figure 9(b) shows that the orientation divergence in ferrite grains after fracture at 153 K is as much as that in the initial structure showed in Fig. 8(b). It suggests that the plastic strain induced into ferrite grains during impact test is very small. Figure 9(c) shows the result of fracture surface trace analysis around a subcrack below the fracture surface on the IPF map. Red cubes describe the orientation of the ferrite phasing subcrack. Most traces correspond to the $\{0\ 0\ 1\}_{BCC}$ plane in which conventional cleavage cracks propagate easily. These crystallographic features of microstructure just below the fracture surface suggest that the fracture at 153 K is a cleavage fracture (CF) propagated into the ferrite + pearlite structure.

Furthermore, **Fig. 10** shows the results of crystallographic features just below the fracture surface failed at 213 K on the middle shelf. In the IPF map in Fig. 10(a), some arrowed ferrite grains clearly contain low angle boundaries. Furthermore, in Fig. 10(b), all measured ferrite grains have large orientation deviation in themselves. This is the concrete evidence that plastic strain was induced around the fracture surface during impact test.

To compare the plastic strain induced into ferrite grains just below the fracture surfaces failed at 213 and 153 K, we evaluated GOS of large ferrite grains whose diameters are over 4.0 μm. **Figure 11** shows the histograms of GOS. GOS of the specimen tested at 153 K increased slightly from that of the initial structure. However, the change was small and their histograms were very similar. On the other hand, the histogram of GOS in the specimen tested at 213 K was completely different from others. That is, it was larger and spread wider than others. This result indicates that the fracture at 213 K on the middle shelf carried large plastic strain. Moreover, it suggests that the fracture on the lower shelf occurred without plastic strain.

4. Discussion

The absorbed energy with fracture, fracture surface, and fracture mode on BCC steel changes with temperature. **Figure 12** shows the conventional model[18] of DBT behavior on BCC steel thick plate. At high temperature, the ductile fracture occurs and makes a plateau in the absorbed energy. This region is called the upper shelf. The fracture surface

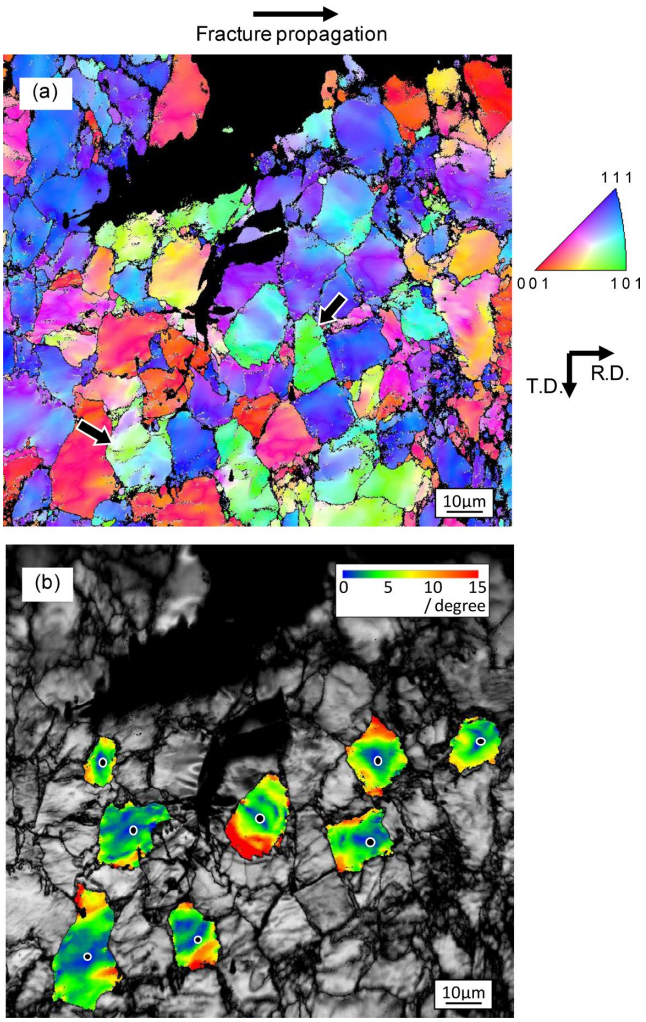

Fig. 10. Orientation image of the ferrite + pearlite steel sheet failed at 153 K in the cross section below the low energy fracture surface. (a) IPF map of ND and (b) misorientation from standard point (●) in each ferrite grain. (Online version in color.)

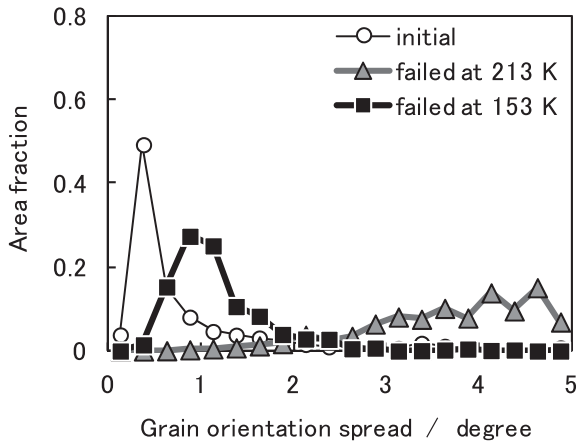

Fig. 11. Influence of impact fracture on the orientation spread in each ferrite grain at each temperature.

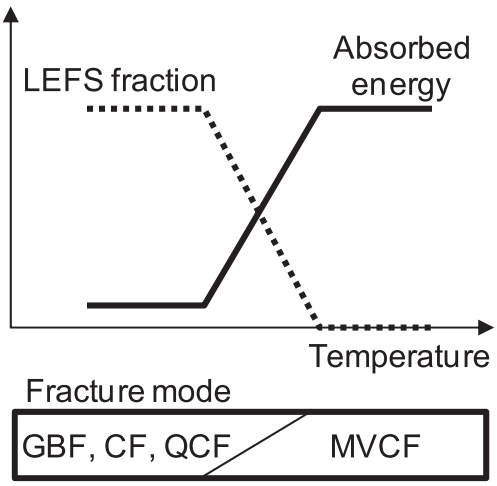

Fig. 12. Schematic of the conventional model for ductile to brittle transition in a BCC steel plate. LEFS: low energy fracture surface, MVCF: microvoid coalescence fracture, GBF: grain boundary fracture, CF: cleavage fracture, and QCF: quasi-cleavage fracture.

on the upper shelf is MVCFS. With decreasing temperature, the absorbed energy decreases continuously until the plateau, which is called the lower shelf. On the lower shelf, brittle fracture occurs and the fracture surface is LEFS. Moreover, it is reported that grain boundary fracture, CF,[20] or quasi-cleavage fracture (QCF)[13,17] occur. The fracture mode changes with material, sample, and other experimental procedures.

On the other hand, **Fig. 13** shows the schematic of DBT behavior observed in this study. The DBT behavior of ferrite + pearlite DP structure steel sheet on Charpy impact test using a sub-size specimen occurred with two step, and it clearly shows the middle shelf. On the upper shelf, the fracture surface is MVCFS, similar to the conventional model. On the middle shelf, the fracture surface is LEFS and the ferrite grains below the fracture surface received plastic strain with or just before fracture. It means that QCF, which is brittle fracture with plastic strain, occurs at the middle temperature. On the lower shelf, the fracture surface is LEFS. However, the fracture occurs without plastic strain. Further, the traces of surfaces around the subcrack corresponding to the $\{0\ 0\ 1\}_{BCC}$ plane. It indicates that CF occurs at low temperature.

During the first transition from the upper shelf to the middle shelf, the fracture mode changes from microvoids coarsening fracture (MVCF) to QCF. Moreover, during the second transition from the middle to the lower shelf, it changes from QCF to CF.

In previous studies, the transition from MVCF to QCF was observed in stainless steel[13] using the Charpy impact test and in spheroidized steel[15] using the tensile test. However, they did not show the two step transition of absorbed energy and the transition from QCF to CF.

Recently, Sirthanakorn *et al.*[19] showed the two step DBT behavior in fully pearlitic steel wires using the impact test with several crosshead speeds. They evaluated that the value of the activation energy associated with the second transition was comparable to that associated with the typical single transition of low carbon ferritic steel. Moreover, they observed the side surfaces near the fractures and showed that the deformation of cementite occurred only at temperatures above the first transition temperature. These results suggest that the second transition is controlled by the DBT behavior in ferrite, which is a softer phase, and that the first transition is controlled by the DBT behavior in cementite, which is a harder phase.

The model assumed from this suggestion is useful to understand the mechanism of the two step DBT behavior with the appearance of QCF. **Figure 14** shows the schematic relation among the yield stresses of ferrite and pearlite, the brittle fracture stress of pearlite, and the DBT temperatures in ferrite + pearlite DP structure steel sheet.[20,21] Pearlite, which is a harder structure in DP steel sheet, has higher yield stress and lower fracture stress than ferrite, which is a softer structure. The yield stresses of ferrite and pearlite ($\sigma_{Y,\alpha}$ and $\sigma_{Y,P}$, respectively) are smaller than the fracture stress of pearlite ($\sigma_{F,P}$) at temperatures above T_1. With the increasing applied stress to the DP structure, ferrite and pearlite undergo plastic deformation separately and successively. Therefore, if ferrite and pearlite have sufficient formability, the fracture occurs in the MVCF mode on the DP structure, which undergoes plastic deformation.

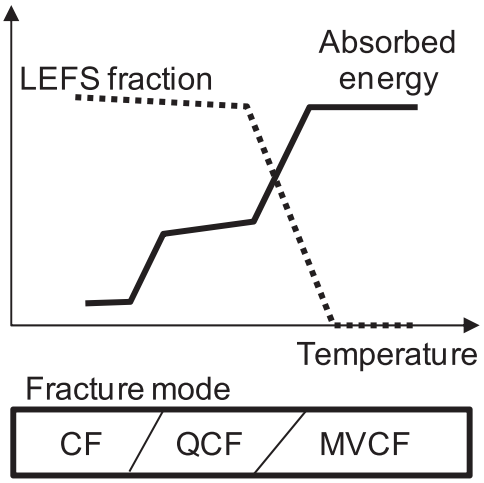

Fig. 13. Schematic of ductile to brittle transition in the ferrite + pearlite steel sheet. LEFS: low energy fracture surface, MVCF: microvoid coalescence fracture, CF: cleavage fracture, and QCF: quasi-cleavage fracture.

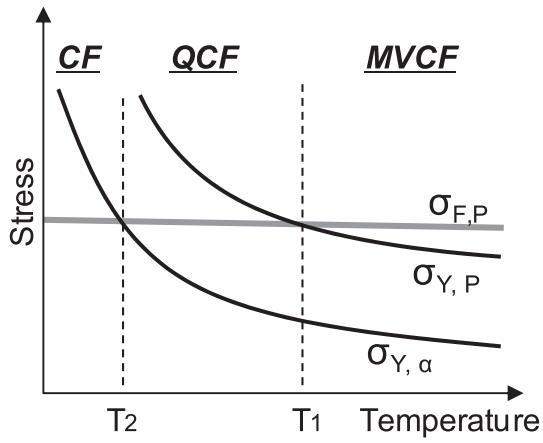

Fig. 14. Schematic relation among the yield stresses, fracture stress, and ductile to brittle transition temperatures in the ferrite + pearlite steel sheet. $\sigma_{F,B}$: the brittle fracture stress of pearlite, $\sigma_{Y,\alpha}$ and $\sigma_{Y,P}$: the yield stresses of ferrite and pearlite, respectively, T_1: the first transition temperature, and T_2: the second transition temperature.

The yield stresses increase with decreasing temperature, and $\sigma_{Y,P}$ becomes higher than $\sigma_{F,P}$ at temperatures below T_1. At temperatures between T_1 and T_2, ferrite begins undergoing plastic deformation first when the applied stress increases and reaches $\sigma_{Y,\alpha}$. Subsequently, the stress applied to pearlite increases continuously with the work hardening of ferrite and reaches $\sigma_{F,P}$ without plastic deformation of pearlite, and the brittle fracture begins to occur in pearlite. If the propagation of the brittle fracture into the ferrite grains, which deform plastically, is easy and does not require dimples, the microstructure near the fracture surface contains ferrite having plastic strain and the fracture surface becomes LEFS. It means that T_1 is the transition temperature of the fracture mode between MVCF and QCF.

At low temperatures below T_2, $\sigma_{Y,\alpha}$ becomes higher than $\sigma_{F,P}$. Because the fracture stress is smaller than both of the yield stresses, the brittle fracture can occur without plastic deformation. In this case, the fracture mode is CF. Therefore, T_2 is the transition temperature of the fracture mode

between QCF and CF.

The model described above seems to be effective for understanding the mechanism of two step DBT behavior in DP steel sheets. This model indicated the important factors that affect the relation shown in Fig. 14: the properties of structures in steel,[9,11,21] strain rate,[19] specimen thickness,[13] and shape of the notch.[13] However, the evidence for the model in this study is not sufficient. It is necessary for the establishment of the DBT model to confirm the starting point of CF and QCF. Furthermore, it is important to investigate the fracture propagation behavior into the ferrite grains, which undergo plastic deformation.

5. Summary

To clarify the impact fracture behavior of ferrite + pearlite DP steel sheets, we examined the Charpy impact test with sub-size specimens and observed fractographs and microstructures just below the fracture surface using the EBSD technique.

(1) During the transition from the upper to the lower shelf, the absorbed energy showed plateau at medium energy between 253 and 193 K. We call this plateau as the "middle shelf."

(2) The fracture surface that failed on the upper shelf is the MVCFS, which is a typical ductile fracture surface. The fracture surfaces that failed on the middle and lower shelf are LEFS, and it is difficult to distinguish them by fractographs.

(3) The ferrite grains just below the fracture surface clearly received plastic strain with fracture on the middle shelf. Moreover, on the lower shelf, they received no or very small plastic strain with fracture.

(4) DBT in this study occurred with two steps. In the first transition, the fracture mode changed from MVCF to QCF. In the second transition, it changed from QCF to CF.

REFERENCES

1) N. Fonstein: Advanced High Strength Sheet Steels, Springer International Publishing, Switzerland, (2015), 3.
2) T. Kunio, M. Shimizu, K. Yamada and H. Suzuki: *Eng. Fract. Mech.*, **7** (1975), 411.
3) M. Calcagnotto, Y. Adachi, D. Ponge and D. Raabe: *Acta Mater.*, **59** (2011), 658.
4) Q. Lai, O. Bouaziz, M. Goune, L. Brassart, M. Verdier, G. Parry, A. Perlade, Y. Brechet and T. Pardoen: *Mater. Sci. Eng. A*, **646** (2015), 322.
5) X. Cai, J. Feng and W. S. Owen: *Metall. Trans. A*, **16A** (1985), 1405.
6) M. Okayasu, K. Sato, M. Mizuno, D. Y. Hwang and D. H. Shin: *Int. J. Fatigue*, **30** (2008), 1358.
7) R. G. Davies: *Metall. Trans. A*, **12A** (1981), 1667.
8) M. Koyama, C. C. Tasan, E. Akiyama, K. Tsuzaki and D. Ponge: *Acta Mater.*, **70** (2014), 174.
9) S. S. M. Tavares, P. D. Pedroza, J. R. Teodósio and T. Gurova: *Scr. Mater.*, **40** (1999), 887.
10) F. Hayat and H. Uzun: *J. Iron Steel Res. Int.*, **18** (2011), 65.
11) M. Calcagnotto, D. Ponge and D. Raabe: *Mater. Sci. Eng. A*, **527** (2010), 7832.
12) A. Pineau: *Int. J. Fract.*, **150** (2008), 129.
13) K. Edsinger, G. R. Odette, G. E. Lucas and J. W. Sheckherd: *J. Nucl. Mater.*, **233**–**237** (1996), 342.
14) A. Uehira and S. Ukai: *J. Nucl. Sci. Technol.*, **41** (2004), 973.
15) A. Kumar, A. J. Wilkinson and S. G. Roberts: *J. Microsc.*, **227** (2007), 248.
16) A. Ayad, N. Allain-Bonasso, N. Rouag and F. Wagner: *Mater. Sci. Forum*, **702**–**703** (2012), 269.
17) G. R. Odette: *J. Nucl. Mater.*, **212**–**215** (1994), 45.
18) G. Krauss: Steels Processing, Structure, and Performance, ASM International, Materials Park, OH, (2005), 201.
19) T. Sirithanakorn, M. Tanaka and K. Higashida: *Mater. Sci. Eng. A*, **611** (2014), 383.
20) J. W. Morris, Jr.: *Mater. Res. Soc. Symp. Proc.*, **539** (1999), 23.
21) T. Hanamura, F. Yin and K. Nagai: *ISIJ Int.*, **44** (2004), 610.